Stem Cell Reports, Volume *2*

Supplemental Information

SIRT1 Is Necessary for Proficient Telomere Elongation and Genomic Stability of Induced Pluripotent Stem Cells

Maria Luigia De Bonis, Sagrario Ortega, and Maria A. Blasco

Inventory of Supplemental Information

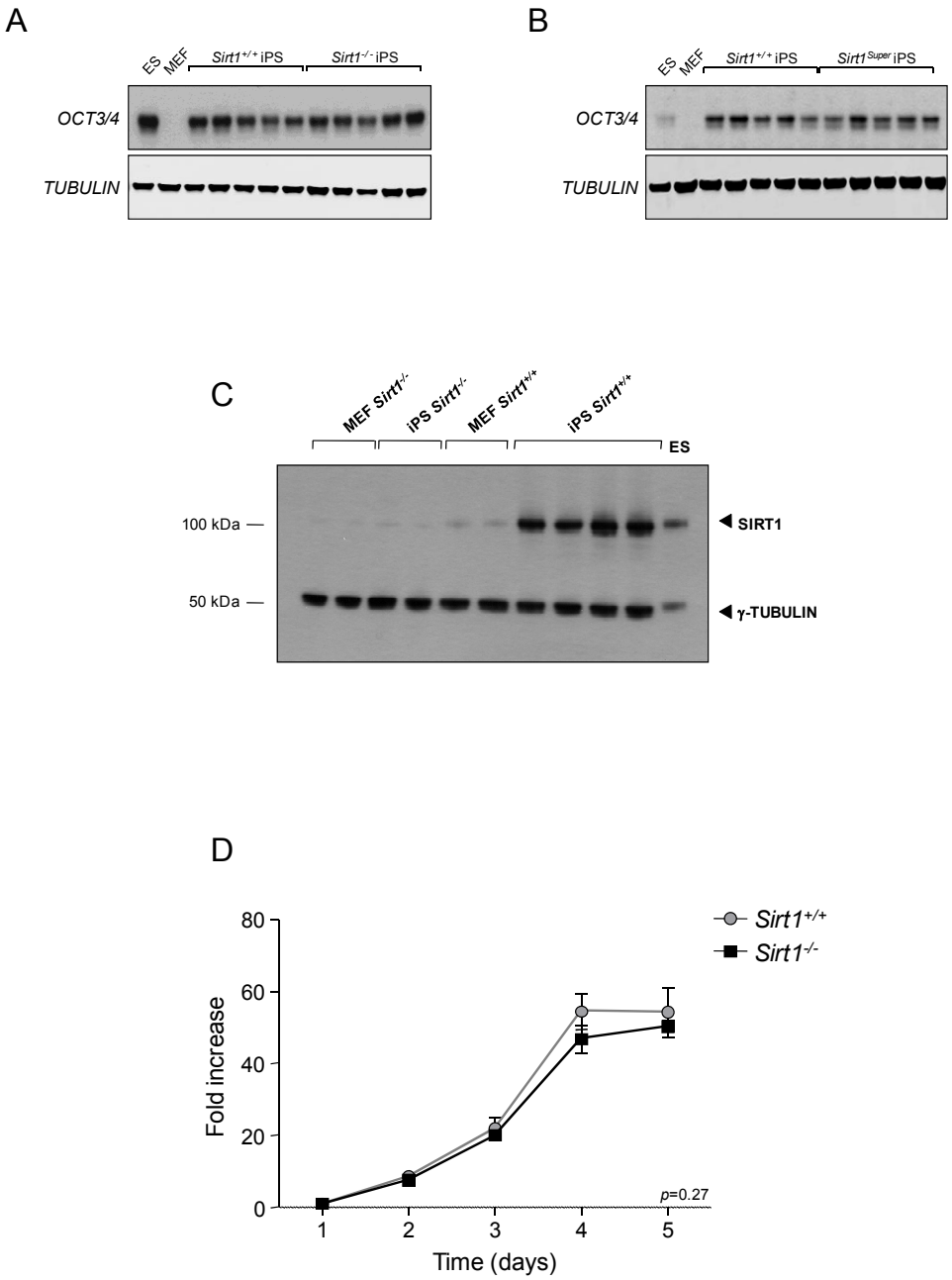

De Bonis *et al.*, Figure S1

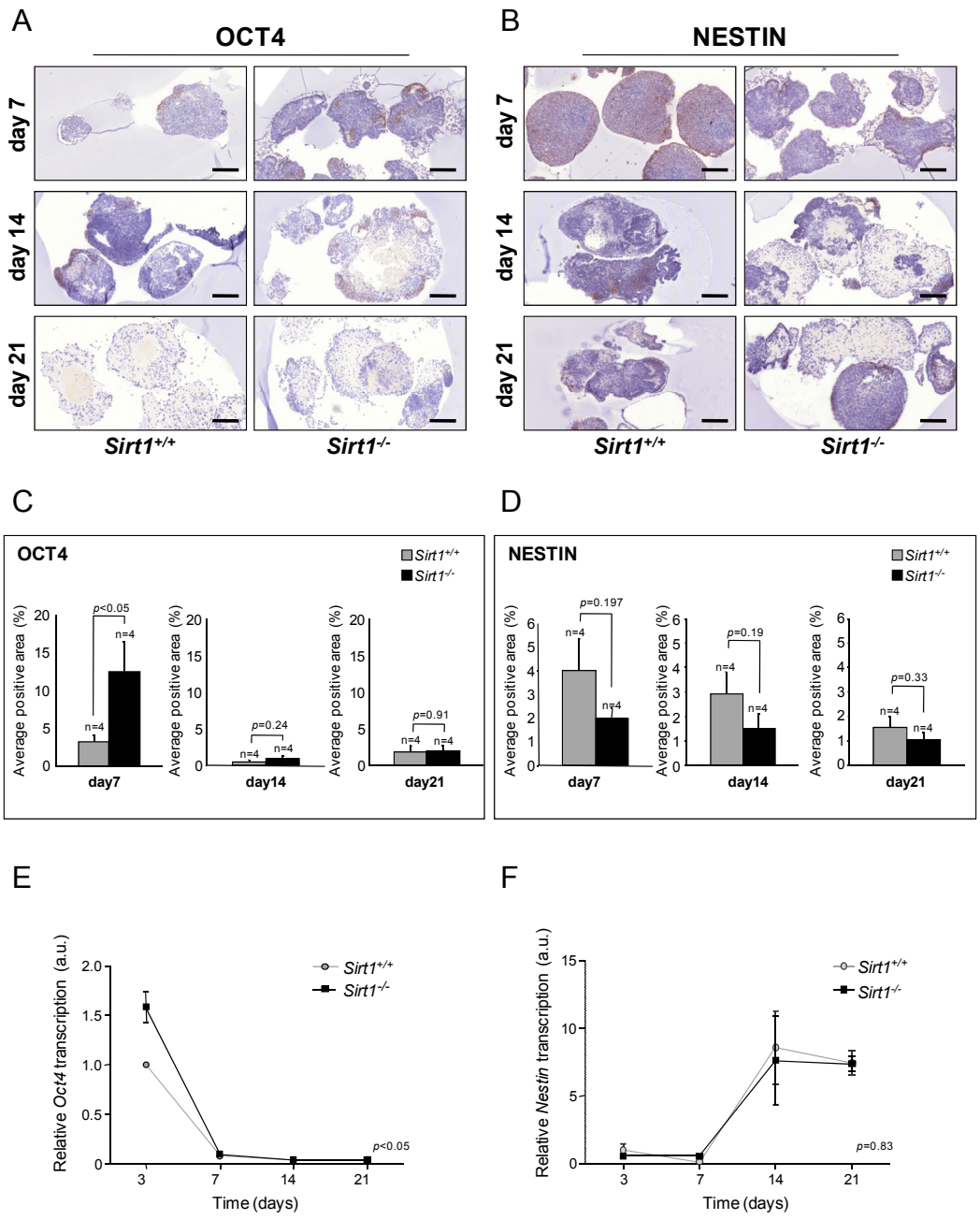

De Bonis *et al.*, Figure S2

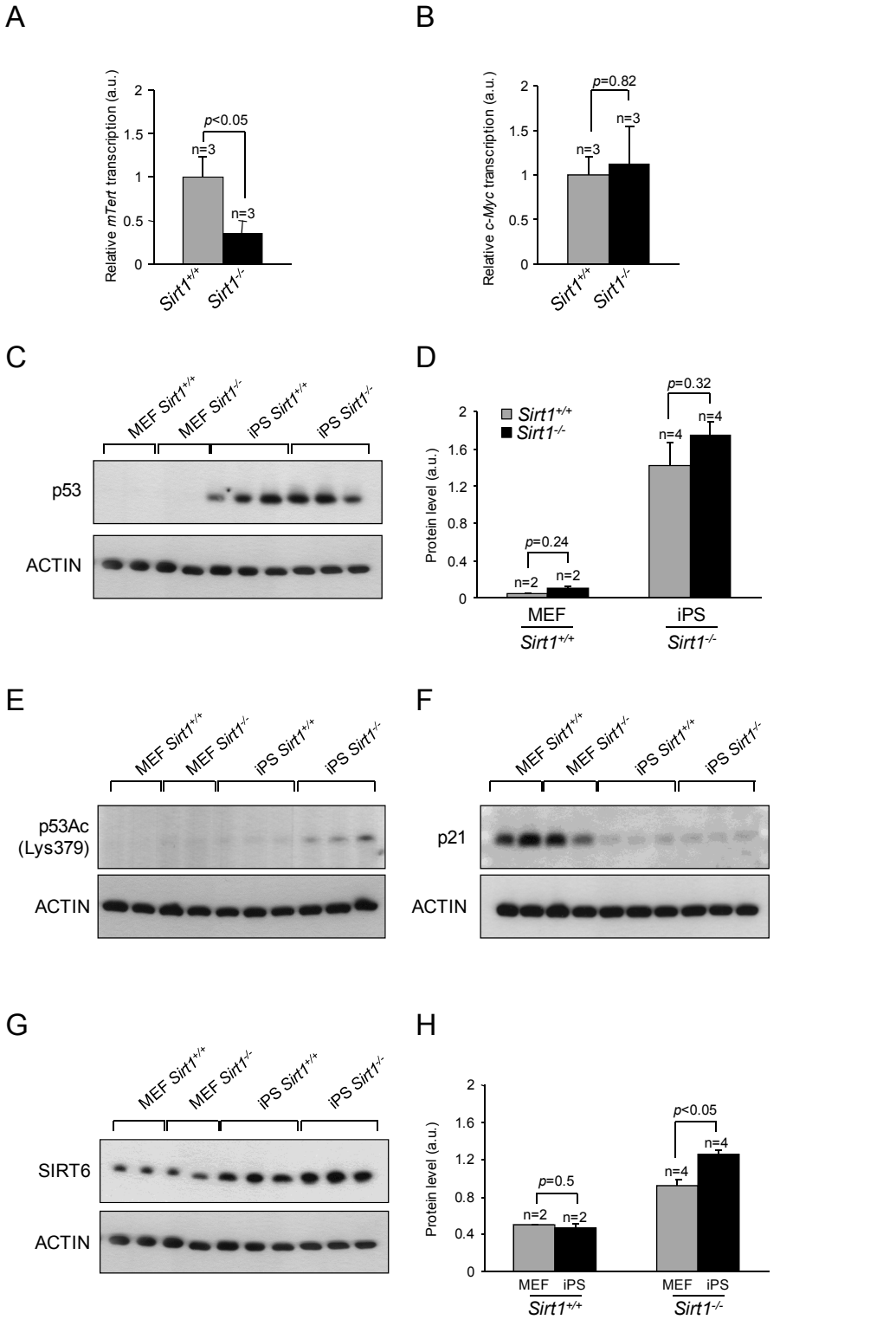

De Bonis *et al.*, Figure S3

	Sex chromosome component	Numerical aberration	Structural aberration	Metaphases (%)	Representative figure
iPS#5-3 (wt)	XY	+2; +8; -16	None	100	A
iPS#9-2 (wt)	X0	+8	None	100	B
iPS#9-3 (wt)	X0	+8 +8 +8	None dup(14) der15 t(15;8)	28.6 42.8 28.6	C D E
iPS#1-1 (ko)	X0	+8; +17x2	rob(6;6); der8 t(8;X)	100	F
iPS#1-2 (ko)	X0	+8 +8	rob(6;6) rob(8;8)	42.8 57.2	G H
iPS#3-1 (ko)	XY X0 X0	None -16 +8	None rob(6;6) rob(8;8)	50 30 20	I J K

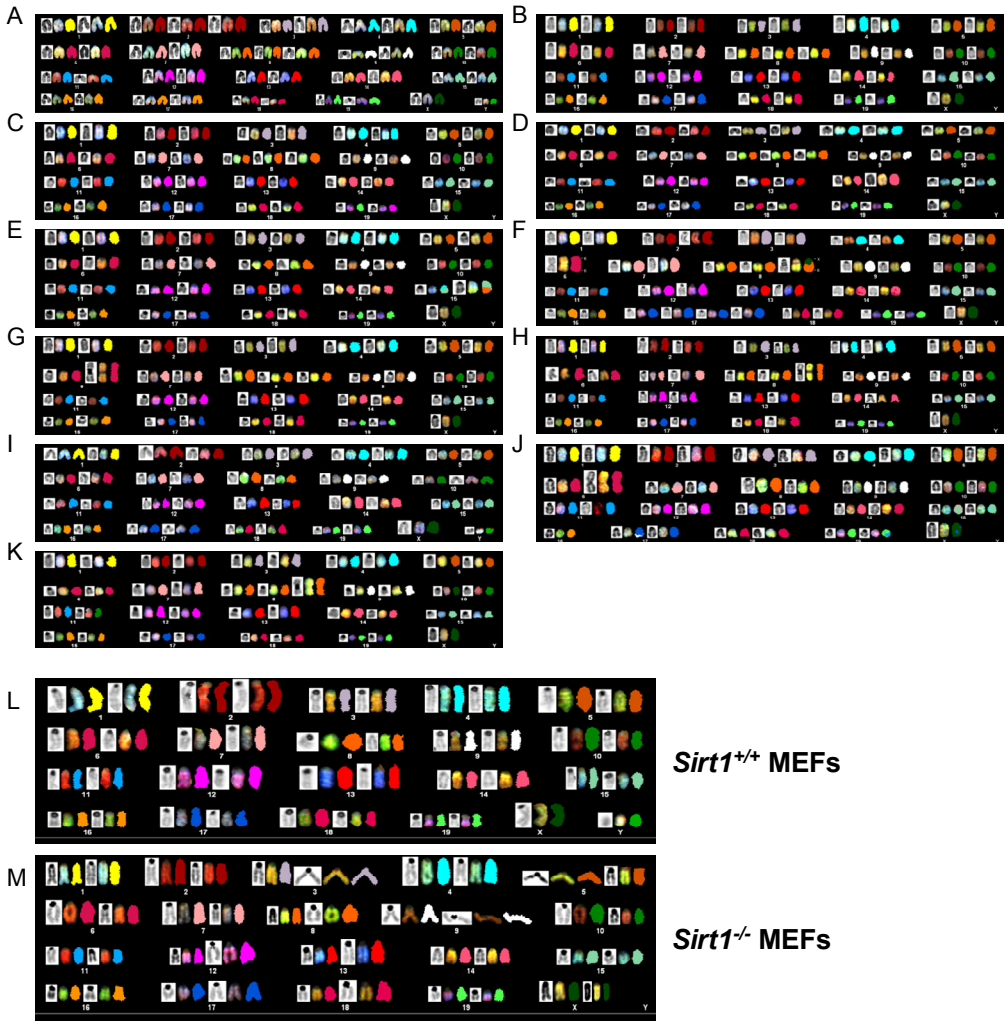

De Bonis *et al.*, Figure S4

Supplemental Figure legends

Figure S1. *Sirt1*$^{-/-}$ iPS proliferate at the same extent than wild-type

(A,B) Western Blot analysis showing the expression of OCT3/4 in *Sirt1*$^{-/-}$ (A) and *Sirt1*^{Super} (B) iPS. Tubulin was included as a loading control. Five individual iPS cell clones per genotype were tested. An ES and a MEF samples were included as positive and negative controls, respectively.

(C) Western Blot analysis showing a robust expression of SIRT1 protein in *Sirt1*$^{+/+}$ iPS. Four individual iPS cell clones were tested. Two independent samples of each *Sirt1*$^{+/+}$ MEFs, *Sirt1*$^{-/-}$ MEFs, and *Sirt1*$^{-/-}$ iPS were also analyzed as a reference. An ES samples was included as a positive control.

(D) Proliferation curves showing that *Sirt1*$^{-/-}$ iPS do not display an intrinsic proliferative advantage compared to their wild-type counterparts. Three individual iPS cell clones per genotype were assayed. The p-value expresses the probability that the two curves are significantly different and has been calculated by a Two-way ANOVA.

Figure S2. *Sirt1*$^{-/-}$ iPS display a delayed exit from pluripotency *in vitro*

(A,B) Representative images of embryoid bodies (EB) sections derived from *Sirt1*$^{+/+}$ or *Sirt1*$^{-/-}$ iPS, stained for OCT4 (A) or NESTIN (B) at the indicated time points after LIF withdrawal. Scale bar 200 μm.

(C,D) The percentage of positive area, quantified by the ImageJ software and normalized to the total EB area in every picture (3 picture per each of 4 clones, a total of 12 picture per genotype), shows that *Sirt1*$^{-/-}$ EBs retain OCT4 positive cells upon LIF withdrawal longer than wild type ones (C), confirming that also *in*

vitro SIRT1 deficiency delays the exit from pluripotency. In line with this observation, although not statistically significant due to variability among samples, *Sirt1*$^{-/-}$ EBs also show a lower percentage of NESTIN positive cells compared to wild-type (D). n indicates the number of independent clones per genotype. Error bars refer to SEM. Statistical analysis was performed using a two-tailed Student's t-test.

(E,F) The transcription of *Oct4* and *Nestin* genes, estimated at different time points (including day3, which has not been analyzed by immunohistochemistry) by quantitative real-time PCR. *Oct4* transcription is significantly higher in *Sirt1*$^{-/-}$ EBs at the earliest time point (E) whereas *Nestin* gene follow the same kinetics over time in EBs of both genotypes (F). p-values express the probability that the two curves are significantly different and have been calculated by a Two-way ANOVA.

Figure S3. p53 expression, acetylation and activity, as well as SIRT6 expression, are not affected by SIRT1 deficiency

(A,B) Transcription of *mTert* (A) and *c-Myc* (B), evaluated by quantitative Real-Time PCR in *Sirt1*$^{-/-}$ versus *Sirt1*$^{+/+}$ iPS at passage 35. Three independent iPS clones per genotype were tested. Error bars refer to SEM. Statistical analysis was performed using a two-tailed Student's t-test.

(C,D) Western Blot analysis showing p53 expression in *Sirt1*$^{+/+}$ and *Sirt1*$^{-/-}$ MEFs and iPS (C). The quantification shows no significant difference in p53 expression in the absence of SIRT1 (D).

(E,F) Western Blot analysis showing the acetylation status of Lys379-p53 protein (E) and p21 expression (F) as a readout of p53 activity in *Sirt1*$^{+/+}$ and *Sirt1*$^{-/-}$ MEFs and iPS.

(G,H) Western Blot analysis showing SIRT6 expression in *Sirt1*$^{+/+}$ and *Sirt1*$^{-/-}$ MEFs and iPS (G). The quantification shows an increase in SIRT6 expression in *Sirt1*$^{-/-}$ iPS, compared with their wild-type counterpart (H). Actin was used as a loading control in each experiment. Two independent MEFs per genotype (n=2) and four independent iPS clones per genotype (n=4) were tested. Error bars refer to SEM. Statistical analysis was performed using a two-tailed Student's t-test.

Figure S4. Spectral karyotyping of *SIRT1* wild-type and knock out iPS

The table summarizes the numerical and structural chromosome aberrations scored in three wild type and three knock out clones through SKY analysis. (A-K). For every subpopulation of metaphases spreads sharing the same karyotype, a representative image is shown. Each chromosome is represented from left to right by DAPI staining, the display color and the classification pseudo-color. (L,M) Example of metaphase spread from *Sirt1*$^{+/+}$ (L) and *Sirt1*$^{-/-}$ (M) parental MEFs analyzed by SKY analysis. The karyotype exhibited by these cells is normal.

Supplemental Experimental Procedures

Cell culture

MEFs (mixed C57BL/6 and 129/Sv genetic background) were cultured in standard DMEM medium with 10% FBS (Gibco). iPS cells were cultured in DMEM (high glucose) supplemented with serum replacement (KSR, Invitrogen), Leukemia Inhibitory Factor (ESGRO Supplement, Millipore) 1000 u/ml, non-essential amino acids, Glutamax and β-mercaptoethanol.

Teratoma formation and generation of chimeras

Nude mice (Crl:Un(Ico)-Foxn1^{nu}) were subcutaneously injected with 2x10^6 cells of each iPS cell clone. Every mouse was injected with *Sirt1*$^{+/+}$ cells on left side and *Sirt1*$^{-/-}$ on right side. Tumor size was measured with a caliber every other day, from day 13 to day 29 post-injection. Tumor volume was calculated according to the formula:

$$\text{Long diameter} \times (\text{short diameter})^2 \times 0.52$$

The ability of the *Sirt1*$^{+/+}$ and *Sirt1*$^{-/-}$ iPS clones to generate chimeras *in vivo* was tested by microinjection into C57BL/6J-Tyr(C-2J)/J (albino) blastocysts, or by aggregation with CD1 (albino) morulae and assessment of hair color in the resulting progeny.

Mice were treated in accordance with the Spanish Laws and the Guidelines for Humane Endpoints for Animals Used in Biomedical Research. The Spanish National Cancer Research Centre (CNIO) is part of the “Carlos III” Health Institute (ISCIII) and all protocols were previously subjected and approved by

the Ethical Committee of the ISCIII; approval ID numbers: PA-311, PA- 352.2 and PA-142/07.

TRF analysis

Cells were included in agarose plugs, and TRF analysis was performed as previously described (Blasco et al., 1997).

Telomere length analysis using telomere Q-FISH on metaphases

Metaphases were prepared from 2 independent MEFs per each genotype and 2 independent clones per each parental MEF. Q-FISH hybridization was performed as previously described (Gonzalo et al., 2006; Samper et al., 2000).

Chromosomal aberrations and SKY analysis

FISH hybridization was performed as described before (Gonzalo et al., 2006; Samper et al., 2000). At least 30 metaphases per genotype were scored for chromosomal aberrations by superimposing the telomere image on the DAPI chromosomes image using the TFL-telo software.

For SKY analysis, metaphase chromosomes were harvested from wild type and knock out iPS cultures (passage 35), according to standard procedures. Slides were freshly prepared from chromosome suspensions stored in fixative (methanol/acetic acid 3:1) at −20°C. Pepsin treatment, hybridization, and detection were carried out according to the protocol provided with the SkyPaint hybridization and detection kit (Applied Spectral Imaging, Migdal Ha'Emek, Israel). Metaphase nuclei were captured at room temperature using the SD300 Spectracube (Applied Spectral Imaging) connected to an Axioplan 2 microscope

(Carl Zeiss Jena GmbH, Jena, Germany). Around 20 metaphases were analyzed for each case using SKYview software (Applied Spectral Imaging). Three independent clones per genotype were analyzed.

ChIP assay

ChIP assays were performed as previously described (Garcia-Cao et al., 2004). In brief, after crosslink and sonication, chromatin from $4x10^6$ cells were used per each immunoprecipitation with protein A/G Plus agarose beads (Santa Cruz Biotechnology, sc-2003) and the following antibodies: 5 μg of anti-histone H3 (#ab1791, Abcam), 8 μl of rabbit polyclonal antibody to TRF1, raised in our laboratory against full-length mouse TRF1 protein, 5 μg of monoclonal anti-HP1γ (#05-690, Upstate Biotechnology), 5 μg of anti-H4K16Ac (#39167, Active Motif) or preimmune serum. The immunoprecipitated DNA was transferred to a Hybond N^+ membrane using a dot blot apparatus. The membrane was then hybridized with either a telomeric probe containing TTAGGG repeats. Quantification of the signal was performed with ImageJ software. The amount of telomeric DNA after ChIP was normalized to the total telomeric or centromeric DNA signal respectively for each genotype (input), as well as to the H3 and H4 abundance at these domains, thus correcting for differences in the number of telomere repeats or in nucleosome spacing.

Telomere transcription

Total RNA was isolated with Trizol (Invitrogen) following the manufacturer' protocol, and subject to Dot blot analysis.

Dot Blot analysis was performed as described (Schoeftner and Blasco, 2008). Briefly, total RNA was prepared using Trizol (Invitrogen), quantified and transferred to a Hybond N^+ membrane using a dot blot apparatus. For detection of TERRA, random primer-labeled (Rediprime, GE Healthcare), a 1.6 Kb (TTAGGG)n cDNA insert, excised from pNYH3 (kind gift from T. de Lange, Rockefeller University, NY), was used. Normalization of Dot blot signals was performed with the 18S rRNA.

List of oligos used in Quantitative Real-Time PCR

- mNanog-for 5’- CAGAAAAACCAGTGGTTGAAGACTAG -3’
- mNanog-rev 5’- GCAATGGATGCTGGGATACTC -3’
- mOct3/4-for 5’- GGCGTTCTCTTTGGAAAGGTGTTC -3’
- mOct3/4-rev 5’- CTCGAACCACATCCTTCTCT -3’
- mGAPDH-RT-for 5’- CCCACTAACATCAAATGGGG -3’
- mGAPDH-RT-rev 5’- CCTTCCACAATGCCAAAGTT -3’
- mTert-for 5’- GGATTGCCACTGGCTCCG -3’
- mTert-rev 5’- TGCCTGACCTCCTCTTCTGGAC -3’
- c-Myc-for 5’- CCTAGTGCTGCATGAGGAG -3’
- c-Myc-rev 5’- CCTCATCTTCTTGCTCTTCTTCA -3’

List of antibodies used in Western Blot

- SIRT1 (1:2000; Abcam ab12193)
- NANOG (1:1000; Chemicon AB 5731)
- OCT4 (1:500; Santa Cruz sc-9081)
- p53 (1:1000; Cell Signaling #2524)
- p53 acetylated (Lys379, 1:1000, Cell Signaling #2570)
- p21 (1:250; Santa Cruz sc-397)
- SIRT6 (1:2000; Millipore #ABE102)
- Tubulin (1:10000 SIGMA T6557)
- Actin (1:10000; Sigma A5441)
- c-MYC (1:1000 Cell Signaling D84C12 #5605)
- mTERT (1:1000 Calbiochem #582005)
- SMC1 (1:1000, Bethyl Laboratories # A300-055A)
- FLAG (1:5000 Sigma #F3165)

Supplemental References

Blasco, M.A., Lee, H.W., Hande, M.P., Samper, E., Lansdorp, P.M., DePinho, R.A., and Greider, C.W. (1997). Telomere shortening and tumor formation by mouse cells lacking telomerase RNA. Cell *91*, 25-34.

Garcia-Cao, M., O'Sullivan, R., Peters, A.H., Jenuwein, T., and Blasco, M.A. (2004). Epigenetic regulation of telomere length in mammalian cells by the Suv39h1 and Suv39h2 histone methyltransferases. Nat Genet *36*, 94-99.

Gonzalo, S., Jaco, I., Fraga, M.F., Chen, T., Li, E., Esteller, M., and Blasco, M.A. (2006). DNA methyltransferases control telomere length and telomere recombination in mammalian cells. Nat Cell Biol *8*, 416-424.

Samper, E., Goytisolo, F.A., Slijepcevic, P., van Buul, P.P., and Blasco, M.A. (2000). Mammalian Ku86 protein prevents telomeric fusions independently of the length of TTAGGG repeats and the G-strand overhang. EMBO Rep *1*, 244-252.